J|A|C|S
ARTICLES
Published on Web 10/11/2006

Peptide-Directed Microstructure Formation of Polymers in Organic Media

Jens Hentschel and Hans G. Börner*

Contribution from the Max Planck Institute of Colloids and Interfaces, MPI KGF Golm, 14424 Potsdam, Germany

Received July 13, 2006; E-mail: hans.boerner@mpikg.mpg.de

Abstract: Synthesis and peptide-guided self-assembly of an organo-soluble peptide−polymer conjugate, comprising a sequence-defined polypeptide and a poly(*n*-butyl acrylate), are described. The amino acid sequence of the peptide encodes a high tendency to adopt an antiparallel β-sheet motif, and thus programs the formation of tapelike microstructures. Easy synthesis and controllable self-assembly is ensured by the incorporation of structure breaking switch defects into the peptide segment. This suppresses temporarily the aggregation tendency of the conjugate as shown by circular dichroism, infrared spectroscopy (FT-IR), and atomic force microscopy (AFM). A pH-controlled rearrangement in the switch segments restores the native peptide backbone, triggering the self-assembly process and leading to the formation of densely twisted tapelike microstructures as could be observed by AFM and transmission electron microscopy. The resulting helical superstructures, when deposited on a substrate, are 2.9 nm high, 10 nm wide, and up to 2.3 μm long. The helical pitch is about 37 nm, and the pitch angle is 48°. The helical superstructures undergo defined entanglement to form superhelices, leading to the formation of soft, continuous organogels. A twisted two-dimensional core−shell tape is proposed as a structure model, in which the peptide segments form an antiparallel β-sheet with a polymer shell.

Introduction

The structural diversity adopted by native polypeptides and proteins is considered as the key factor of their enormous functional variety.[1] Structure formation in protein systems occurs via specific interactions as encoded in the monomer sequence of linear polypeptide chains by a code of 20 different amino acids. Considering this, the concepts applied in synthetic polymer chemistry to induce and control organization processes and direct the formation of microstructures are rather simple.[2−4]

Recently, considerable efforts have been devoted to both mimicking biological structure formation processes and utilizing these principles for structuring synthetic polymers.[5−8] Besides the exploitation of the hybridization of oligonucleotides[9,10] or oligo(peptide−nucleotides),[11] focus has been particularly directed to the self-assembly of oligopeptides. The latter prospectively exhibits the potential to enhance the structural and functional space available for polymer assemblies and indeed might allow for the rational design of hierarchically ordered (nano)structures.[5] Moreover, polypeptides have the potential to interact with complex biological systems. Hence, they may combine self-assembly properties with the capability to communicate at the interface between synthetic materials and biosystems, making bio-active assemblies attainable.[12]

The peptide-guided organization of synthetic polymers to induce and control the formation of microstructures has been demonstrated with peptide−polymer conjugates. A variety of oligopeptides, capable of specific self-organization, were conjugated to synthetic polymers as blocks,[13−17] multiblocks,[18,19] or grafts.[20,21] Driven by the assembly of these peptide segments, microstructure formation was induced in the synthetic polymer. Among the specific organization motifs, the coiled-coil,[16,17] the β-sheet,[13−15,22−24] or the elastin structure motif[20] have been utilized. However, until now, only water-soluble polymers such

(1) Creighton, T. E. *Proteins: Structures and Molecular Properties*, 2nd ed.; W. H. Freeman: New York, 1993; 512 pp.
(2) Bates, F. S.; Fredrickson, G. H. *Phys. Today* **1999**, *52*, 32−38.
(3) Förster, S.; Konrad, M. *J. Mater. Chem.* **2003**, *13*, 2671−2688.
(4) Förster, S.; Plantenberg, T. *Angew. Chem., Int. Ed.* **2002**, *41*, 688−714.
(5) Whitesides, G. M. *Small* **2005**, *1*, 172−179.
(6) Fratzl, P. *Curr. Opin. Colloid Interface Sci.* **2003**, *8*, 32−39.
(7) Zhao, X.; Zhang, S. *Trends Biotechnol.* **2004**, *22*, 470−476.
(8) Zhang, S. *Nat. Biotechnol.* **2003**, *21*, 1171−1178.
(9) Watson, K. J.; Park, S. J.; Im, J. H.; Nguyen, S. T.; Mirkin, C. A. *J. Am. Chem. Soc.* **2001**, *123*, 5592−5593.
(10) Gibbs, J. M.; Park, S.-J.; Anderson, D. R.; Watson, K. J.; Mirkin, C. A.; T., N. S. *J. Am. Chem. Soc.* **2005**, *127*, 1170−1178.
(11) Cao, R.; Gu, Z. Y.; Hsu, L.; Patterson, G. D.; Armitage, B. A. *J. Am. Chem. Soc.* **2003**, *125*, 10250−10256.
(12) Tirrell, M.; Kokkoli, E.; Biesalski, M. *Surf. Sci.* **2002**, *500*, 61−83.
(13) Burkoth, T. S.; Benzinger, T. L. S.; Urban, V.; Lynn, D. G.; Meredith, S. C.; Thiyagarajan, P. *J. Am. Chem. Soc.* **1999**, *121*, 7429−7430.
(14) Eckhardt, D.; Groenewolt, M.; Krause, E.; Börner, H. G. *Chem. Commun.* **2005**, 2814−2816.
(15) Hentschel, J.; Krause, E.; Beyermann, M.; Börner, H. G. *J. Am. Chem. Soc.* **2006**, *128*, 7722−7723.
(16) Vandermeulen, G. W. M.; Tziatzios, C.; Klok, H. A. *Macromolecules* **2003**, *36*, 4107−4114.
(17) Pechar, M.; Kopeckova, P.; Joss, L.; Kopecek, J. *Macromol. Biosci.* **2002**, *2*, 199−206.
(18) Rathore, O.; Winningham, M. J.; Sogah, D. Y. *J. Polym. Sci., Part A: Polym. Chem.* **2000**, *38*, 352−366.
(19) Rosler, A.; Klok, H. A.; Hamley, I. W.; Castelletto, V.; Mykhaylyk, O. O. *Biomacromolecules* **2003**, *4*, 859−863.
(20) Ayres, L.; Vos, M. R. J.; Adams, P.; Shklyarevskiy, I. O.; van Hest, J. C. M. *Macromolecules* **2003**, *36*, 5967−5973.
(21) Ayres, L.; Adams, P. H. H. M.; Loewik, D. W. P. M.; Van Hest, J. C. M. *Biomacromolecules* **2005**, *6*, 825−831.
(22) Hamley, I. W.; Ansari, I. A.; Castelletto, V.; Nuhn, H.; Rosler, A.; Klok, H. A. *Biomacromolecules* **2005**, *6*, 1310−1315.

10.1021/ja0649872 CCC: $33.50

Scheme 1. Synthesis of the Peptide Polymer Conjugate[a]

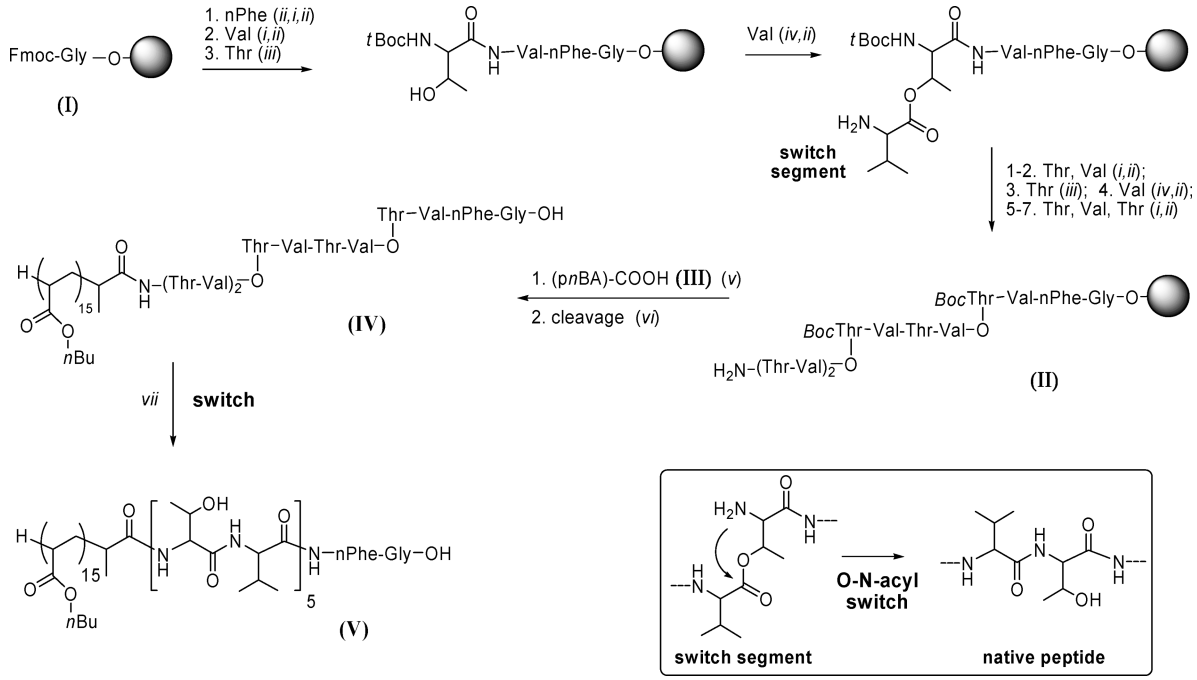

[a] Reagents and conditions: 2-chloro-trityl chloride TentaGel-polystyrene resin loaded with Fmoc−Gly OH (I); (i) Fmoc−Aa, HBTU/DIPEA/NMP, 20 min; (ii) 20 vol % piperidine/NMP; (iii) Boc−Thr OH, HBTU/DIPEA/NMP, 20 min; (iv) Fmoc−Val OH, DIC/NMI/DCM, 2 × 2 h; (v) PyBOP/HOBt/DIPEA/DMF, 2 × 18 h; (vi) 30 vol % TFA/DCM; (vii) addition of base (O → N acyl switch as outlined in the inset).

as poly(ethylene oxide) were applied and the self-assembly process was performed in the native, aqueous environment of polypeptides. This strongly limits the pool of suitable synthetic polymers and thus the diversity of structured materials that can be realized.

Here, we extend the approach of peptide-guided microstructure formation of synthetic polymers to organic media, and hence allow the integration of an array of organo-soluble, synthetic polymers.[25,26] Therefore, this route might give access to a variety of polymeric materials with a defined hierarchical microstructure, formed via processes that are facilitated by specific polypeptide assembly.

Results and Discussion

To demonstrate the peptide-guided organization in organic solvents, a linear AB-block copolymer, comprising a synthetic polymer block and a monodisperse, sequence-defined oligopeptide segment, was synthesized. The organo-soluble poly(*n*-butyl acrylate) (p*n*BA) was chosen as the synthetic polymer block due to its amorphous character and a low T_g. This polymer provides a suitable model, because polymer crystallization or glass formation is not expected to interfere with the peptide self-organization process. Moreover, poly((meth)acrylates) are an important polymer platform for both academic and applied industrial research. Their broad range of functional and mechanical properties allows covering applications from, for example, glues over Plexiglas windows to polymer carriers for therapeutics.

As is outlined in Scheme 1, the peptide−polymer conjugate was obtained using solid-phase supported synthesis techniques. After stepwise amino acid assembly to build up the peptide segment (**II**), an end-functional polymer block (**III**) was coupled to the N-terminus of the supported peptide (**IV**). This coupling approach allows an easy characterization of both the peptide segment and the polymer block separately and ensures the synthesis of a well-defined conjugate.

Synthesis of the Peptide Segment. The peptide segment of the conjugate was designed to control the aggregation process and to direct the formation of the microstructure. Therefore, a high tendency to self-organize into a well-defined tape structure was encoded into the amino acid sequence. This was realized by the peptide $(Thr-Val)_5-nPhe-Gly$ (Scheme 1, **II**) where Thr = threonine, Val = valine, Gly = glycine, and nPhe = 4-nitrophenylalanine. The peptide possesses a $(Thr-Val)_5$-domain ($(TV)_5$) that is known to have high propensities to adopt a stable β-sheet secondary structure in water.[27−29] This aggregator domain was extended on the C-terminal side by a nPhe−Gly sequence, contributing to solubility and providing the 4-nitrophenylalanine as a spectroscopic marker for ease of quantitative analysis.

The solid-phase supported peptide synthesis (SPPS) of peptides with a high tendency to aggregate, such as a $(TV)_5$-domain, is considered to be highly difficult,[30] primarily because aggregation occurs during synthesis, analysis, and polymer conjugation. To overcome these synthetic obstacles, two well-

(23) Smeenk, J. M.; Otten, M. B. J.; Thies, J.; Tirrell, D. A.; Stunnenberg, H. G.; van Hest, J. C. M. *Angew. Chem., Int. Ed.* **2005**, *44*, 1968−1971.
(24) Collier, J. H.; Messersmith, P. B. *Adv. Mater.* **2004**, *16*, 907−910.
(25) Rettig, H.; Krause, E.; Boerner, H. G. *Macromol. Rapid Commun.* **2004**, *25*, 1251−1256.
(26) ten Cate, M. G. J.; Rettig, H.; Bernhardt, K.; Boerner, H. G. *Macromolecules* **2005**, *38*, 10643−10649.
(27) Janek, K.; Behlke, J.; Zipper, J.; Fabian, H.; Georgalis, Y.; Beyermann, M.; Bienert, M.; Krause, E. *Biochemistry* **1999**, *38*, 8246−8252.
(28) Xiong, H. Y.; Buckwalter, B. L.; Shieh, H. M.; Hecht, M. H. *Proc. Natl. Acad. Sci. U.S.A.* **1995**, *92*, 6349−6353.
(29) Altmann, K. H.; Florsheimer, A.; Mutter, M. *Int. J. Pept. Protein Res.* **1986**, *27*, 314−319.
(30) Quibbel, M.; Johnson, T. *Difficult peptides. Fmoc Solid-Phase Peptide Synthesis. A Practical Approach*; OUP: Oxford, 2000; pp 115−136.

defined defect segments,[31,32] referred to as "switch" segments[33] (Scheme 1, inset), were incorporated into the peptide sequence. These two defects were located at sequence positions between the Val[4]−Thr[5] and the Val[8]−Thr[9] (O^{β} derivative of Thr[5] and Thr[9]; Scheme 1, **II**) and exhibit an ester connectivity between the Val^{n} and the Thr^{n+1} instead of the native amide linkage. This was achieved by connecting the carboxylate of the valine$^{(n)}$ not to the α-amine but rather to the β-hydroxyl group of the threonine$^{(n+1)}$ (cf., Scheme 1 inset and structure **II**)). Recently, an all-switch $(TV)_5$-domain was synthesized,[15] showing switch-ester defects in each Val−Thr repeat and proving that such structures effectively suppress the aggregation tendency in water.[15] Even if a fully automated synthesis of switch segments might be possible, it is not recommended because quantitative formation of the switch ester segment should be verified in each coupling step. Thus, to allow for a convenient semi-automated synthesis, a 1,3-switch peptide, exhibiting alternating repeats of native and switch Val−Thr segments, was synthesized. After a small fraction of the peptide **II** was cleaved from the support, the chemical structure was characterized by means of electrospray mass spectrometry (ESI-MS) and ^{1}H NMR. ESI-MS measurements show the appropriate mass signal at m/z 1291 that could be assigned to $[M + Na]^+$ (m_{th} = 1291.4 Da) with an accuracy of ±0.4 Da (cf., Supporting Information). Moreover, ^{1}H NMR confirms the structural identity of **II** by showing the presence of two switch threonine esters (δ = 1.32 ppm; C(CH_3)O−CO), three native threonine amides (δ = 1.15−1.21 ppm; C(CH_3)OH), and five valine residues (δ = 2.02−2.18 ppm; CH(CH_3)$_2$) with respect to the resonances of the nPhe (δ = 7.52 and 8.13 ppm; $C_{ar}H$).

Synthesis of the Peptide−Polymer Conjugate. Subsequently, the end-functionalized p*n*BA block was conjugated to the N-terminus of the supported peptide (Scheme 1). For this step, a p*n*BA, exhibiting only one terminal carboxyl functionality, was synthesized via atom transfer radical polymerization (ATRP[34]) of *n*-butyl acrylate using α-bromo-propionic acid benzyl ester as an initiator. The benzyl ester group can be selectively cleaved via reductive means while preserving the acrylate ester moieties. Furthermore, under these conditions, the ω-bromo functionality of the polymer, which might otherwise cause side reactions during conjugation, is removed. The resulting polymer **III** was characterized by means of gel permeation chromatography (GPC), ^{1}H NMR, and MALDI-TOF-MS. These methods show a $M_{n,GPC}$ = 2300 (DP_n = 18; M_w/M_n = 1.13) and verify the selective end-functionalization of **III**.

Polymer **III** was coupled to the N-terminus of the supported **II** by following enforced coupling protocols using PyBOP in DMF. Quantitative conjugation was confirmed by a negative Kaiser test that indicated the absence of free amine groups. After liberation of the conjugate **IV** from the support, the product was precipitated, dried in a vacuum, freeze-dried from dioxane, and isolated in about 62% yield. Quantitative attachment of the p*n*BA to the peptide segment was verified, within the experimental error, by ^{1}H NMR measurements. These show the expected ratio of *n*BA repeat units to the peptide segment of 16:1 by comparing the resonances δ = 1.41 and 7.54 ppm characteristic for the polymer (CH_2−CH_3) and peptide segments ($C_{ar}H$, nPhe), respectively. Moreover, this suggests that an obvious amount of saponification of the p*n*BA−ester groups was not occurring during cleavage and isolation of **IV**.

Microstructure Formation of the Peptide−Polymer Conjugate. The obtained conjugate **IV** was soluble in diverse organic solvents including methanol, THF, and chloroform, without showing structure formation due to peptide self-organization. Recently, it has been shown with a peptide−polymer conjugate, which combines poly(ethylene oxide) and an all-switch $(TV)_5$-domain, that the switch segments are stable in aqueous solution below pH ≤ 6.[15] This was explained by the fact that the α-amine groups of the threonine switch moieties are fully protonated under these conditions, forming a nonnucleophilic α-ammonium. An increase of the pH shifts the protonation equilibrium from the ammonium to the nucleophilic amine and triggers a regioselective rearrangement in the switch segments (O → N acyl transfer, cf., inset in Scheme 1) that leads to the formation of the continuous native peptide backbone.

An analogous transition from the peptide segment with switch defects, showing suppressed aggregation behavior to the native peptide with high aggregation tendency, can be expected for the 1,3-switch system in organic solvents. This was demonstrated by circular dichroism spectroscopy (CD) (cf., Supporting Information). A solution of the nonswitched **IV** in methanol shows a CD-adsorption minimum around 195 nm and a broad maximum around 215 nm. While the latter signal is characteristic for the switch defects, the CD-minimum results from the native peptide segments, which adopt a statistical chain-segment conformation. No indications of peptide secondary structure formation were observed under these conditions over longer time periods. This highlights that the effective structure-disturbing properties of the switch defect segments are also present in organic solvents. After the apparent pH value of the solution was adjusted to about 7.5 by the addition of methanolic NaOH, the typical CD cotton effects for β-sheets were observed within 10−40 min. This transition demonstrates a rapid restoring of the self-assembly properties of the peptide segment and, hence, an effective switch from **IV** to **V** (cf., Supporting Information).

However, the formation of well-defined microstructures could not be observed by atomic force microscopy (AFM) (cf., Supporting Information). This probably can be explained by a more dynamic β-sheet formation process of $(TV)_5$-domains in methanol in comparison to that in water. Because of the absence of the hydrophobic effect in methanol, the strongest driving force for the stabilization of β-sheets is missing, resulting in the formation of more or less transient β-sheet associates. In protic organic solvents as compared to water, the association free energy of isolated conjugates, which assemble into β-sheets, mainly results from the small differences in H-bond energies between the peptide/solvent (dissociated form) and the peptide/peptide (associated form). Because the loss in conformational entropy of the conjugate during aggregation must be at least counterbalanced, the overall stability of β-sheets is comparatively low. This is consistent with the CD investigations, showing that the self-organization process of **V** in methanol

(31) Sohma, Y.; Sasaki, M.; Hayashi, Y.; Kimura, T.; Kiso, Y. *Chem. Commun.* **2004**, 124−125.
(32) Carpino, L. A.; Krause, E.; Sferdean, C. D.; Schuemann, M.; Fabian, H.; Bienert, M.; Beyermann, M. *Tetrahedron Lett.* **2004**, *45*, 7519−7523.
(33) Mutter, M.; Chandravarkar, A.; Boyat, C.; Lopez, J.; Dos Santos, S.; Mandal, B.; Mimna, R.; Murat, K.; Patiny, L.; Saucede, L.; Tuchscherer, G. *Angew. Chem., Int. Ed.* **2004**, *43*, 4172−4178.
(34) Matyjaszewski, K.; Xia, J. H. *Chem. Rev.* **2001**, *101*, 2921−2990.

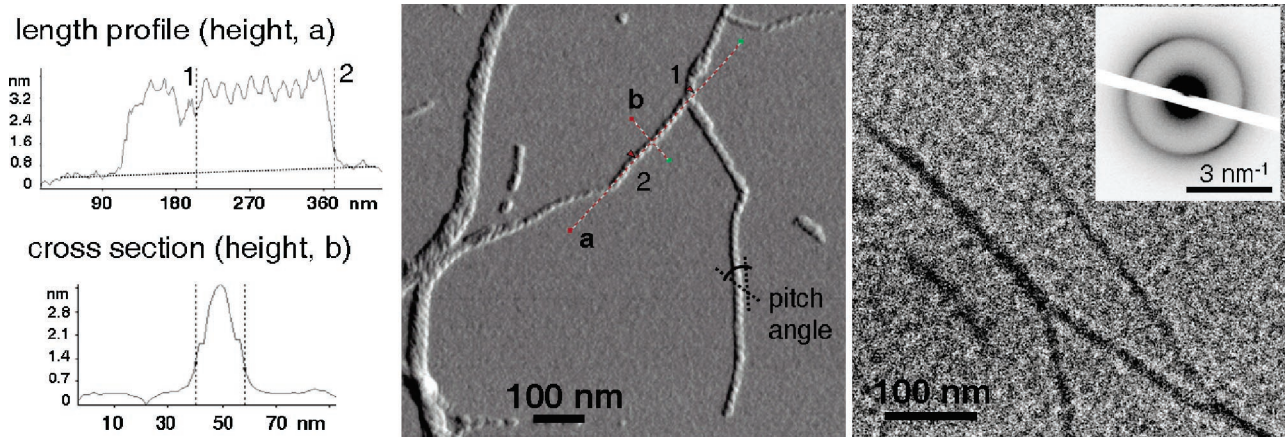

Figure 1. Helical superstructures formed by spontaneous self-assembly of **V** in diethyl ether/methanol (85 vol %, c[**V**] = 0.6 mmol/L, 12 h, room temperature): profiles of the structures from AFM height image corresponding to the middle image (left); AFM micrograph (tapping mode, phase image $z = 10°$, spin-coated solution of **V** 10× diluted) (middle); and TEM image (unstained, 10× diluted) including SAED from a representative area as inset (right).

proceeds with a moderate rate, because the maximum intensity of CD absorbance at 216 nm was reached only after about 24 h. Moreover, it has been described previously that methanol strongly slows down the self-assembly process of β-sheet forming peptides, even of those exhibiting a very high aggregation tendency.[14]

To increase the strength of hydrogen bonds that primarily stabilize the β-sheets in organic solvents, the methanol was substituted by diethyl ether. However, to preserve dynamics in the peptide organization process to allow auto correction and hence prevent the kinetic trapping of aggregates in local energy minima, 15 vol % of methanol was added as a cosolvent.

The nonswitched conjugate **IV** was readily soluble in diethyl ether/methanol. No peptide-directed organization occurred, as indicated by AFM, showing no evidence of distinct microstructures (cf., Supporting Information). This was confirmed by FT-IR measurements of thin films, obtained by solvent evaporation, indicating that the peptide segments do not adopt a secondary structure motif. The amide I band at $\nu = 1641$ cm^{-1} remains unchanged as compared to the undissolved **IV** and is in good agreement with disturbed (TV)-multimer peptides that adopt a statistical chain segment conformation.[27] Moreover, the switch ester groups are visible and stable as indicated by the characteristic O^{sec}−ester band at $\nu = 1780$ cm^{-1}.

The addition of 1 equivalent of methanolic NaOH with respect to the switch defects rapidly triggers the rearrangement in the switch segments and restores the active $(TV)_5$-aggregator domain. This was verified by FT-IR, showing the disappearance of the switch ester absorption band and the shift of the main amide I absorption band to $\nu = 1633$ cm^{-1} (cf., Supporting Information). The latter and the bands at $\nu = 1660$ cm^{-1} and $\nu = 1690$ cm^{-1} are typical vibrational modes for a peptide that adopts an antiparallel β-sheet; this is consistent with literature examples, describing, for example, the self-assembly of model $(TV)_5$-peptides.[27,29] As compared to these model oligopeptides, the formation of an antiparallel β-sheet is even more likely for a polymer−peptide conjugate because this assembly allows the minimization of the steric repulsion of neighboring polymer coils. Furthermore, as explained above, the peptide self-assembly in organic solvents is driven by hydrogen-bond formation, and thus a parallel β-sheet would be disfavored due to H-bond distortions.[1]

In agreement with the IR measurements that suggest peptide organization, AFM has shown the presence of well-defined microstructures, rapidly after performing the switch from **IV** to **V** in diethyl ether/methanol (Figure 1). Densely wound helical superstructures are evident in the AFM micrograph, obtained by spin coating a solution of **V**, 3 h after switching. It is noteworthy that similar structures with a smaller length could be observed already 1 h after switching (data not shown). This suggests a rapid aggregation process and longitudinal structure growth. The observed structures appear to consist of twisted and bent β-sheet tapes. This hypothesis is supported by FT-IR spectroscopy, because the absorption band at $\nu = 1660$ cm^{-1} can be correlated to extended β-sheets that show a distortion into large loop structures.[35] Moreover, the presence of β-sheets in these helical superstructures was directly proven by selected area electron diffraction (SAED) during transmission electron microscopy (TEM). A d spacing of 4.72 Å was found, which is typical for interstrand distance of peptides in extended β-sheets (Figure 1, inset right).

The observed biaxial distortion (twist and bend) of β-sheets is frequently described, for instance, for the assembly of oligopeptides[36,37] and, hence, the superstructures are consistent with peptide assembly models.[37] It is noteworthy that all structures show a distinct left-handed helical twist. This is expected for peptide assemblies, because the chirality of L-amino acid building blocks produces a right-handed peptide β-strand that gives rise to a left-handed twist around the long axes of the β-sheet tape.[37]

AFM measurements of the helical superstructures deposited on a substrate show rather uniform height maxima of 2.9 ± 0.5 nm and lengths of up to 2.3 μm (Figure 1). The width of these structures was determined by TEM to be about 10 ± 1 nm (Figure 1). This can be rationalized with a simplified model that describes the structure as a deformed cylinder with elliptical cross section. The helical pattern of the assembly could not be resolved with TEM, supporting a densely wound helix (Figure 1). This indicates that the peptide and the polymer exhibit neither

(35) Surewicz, W. K.; Mantsch, H. H.; Chapman, D. *Biochemistry* **1993**, *32*, 389−394.
(36) Zhang, S. G. *Biotechnol. Adv.* **2002**, *20*, 321−339.
(37) Aggeli, A.; Nyrkova, I. A.; Bell, M.; Harding, R.; Carrick, L.; McLeish, T. C. B.; Semenov, A. N.; Boden, N. *Proc. Natl. Acad. Sci. U.S.A.* **2001**, *98*, 11857−11862.

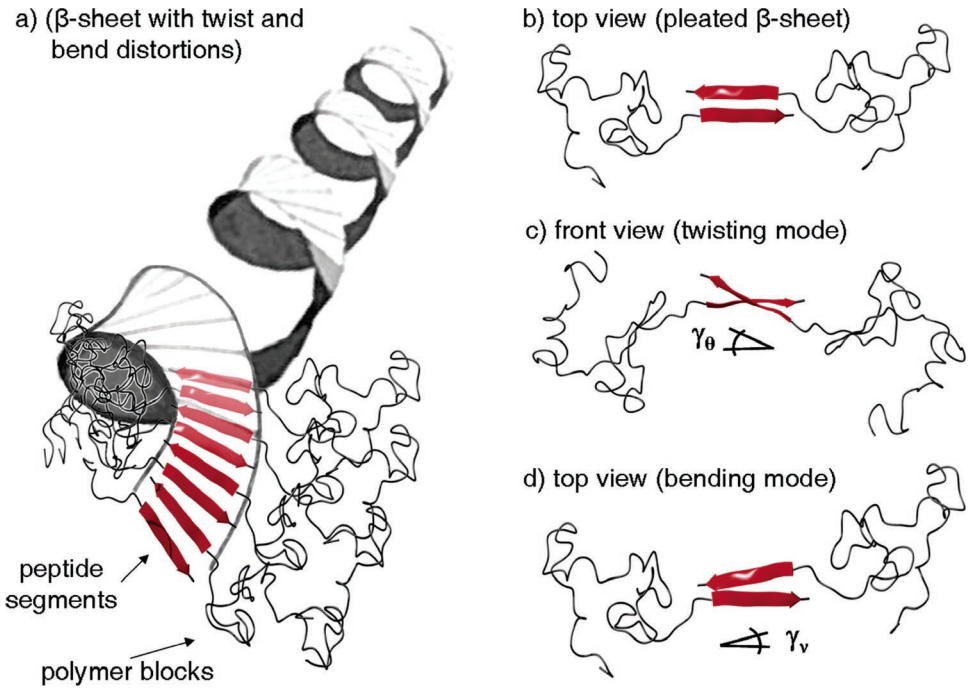

Figure 2. Idealized structure model (a), where the peptide segments of the peptide−p*n*BA conjugate adopt an antiparallel β-sheet tape (a, front) that shows twist and bend distortions, winding into a helical superstructure (a, back; the polymer coils are not shown due to clarity reasons); and β-sheet distortion modes of model dimers: flat (pleated) sheet ($\gamma_\theta = \gamma_\nu = 0$; Pauling and Corey sheet; (b)), twisted sheet ($\gamma_\theta > 0$ and $\gamma_\nu = 0$; (c)), and bent sheet ($\gamma_\theta = 0$ and $\gamma_\nu > 0$; (d)). (The helical structure of (a) was adapted from ref 37 and reprinted with permission. Copyright 2001 National Academy of Sciences.)

sufficient contrast, nor sufficiently different chemical properties, to allow selective staining. However, the viscoelastic contrast between the peptides, adopting the "2D crystalline" β-sheet, and the low T_g polymer allows visualization with AFM using the phase imaging mode (Figure 1). This permits the precise determination of the helical pitch of about 37.4 ± 3 nm and the rather uniform pitch angle of 48° ± 3°.

On the basis of the observations described above and on literature describing, on one hand, the aggregation behavior of β-sheet forming oligopeptides in organic solvents,[38] and, on the other hand, the assembly of peptide-polymer conjugates in aqueous medium,[14,15,22] a preliminary model can be suggested. As outlined in Figure 2a, the formation of a tape structure is driven by the self-assembly of the oligopeptide segments into an antiparallel β-sheet. This 2D-tape exhibits a semiflexible peptide β-sheet core and a soft p*n*BA shell. Because of the accumulation of residual dipole moments, a flat β-sheet (Figure 2b) is energetically unfavored,[37,39] particularly in an organic solvent with comparatively low dielectric constant. Thus, a left-handed twist is induced, rotating each peptide segment around the long axis of the β-sheet (Figure 2c). Simultaneously with this twist, a bending of the β-sheet tape (Figure 2d) is required to realize the observable helical superstructure (Figure 2a). The appearance of bending in a β-sheet tape is consistent with the self-assembly of model peptides.[37,39,40] It has been suggested that the bending is induced by the different chemical properties of the upper and the lower faces of the β-sheet tape. These chemically asymmetric faces are generated because all threonine side chains of the peptide segments are grouped on one face of the β-sheet, whereas the valine side chains can be found on the other face.[41] The differences in the chemical structure of these faces give rise to a cylindrical curvature, causing the tape to bend into the helical conformation. Probably, this facilitates the formation of H-bonds between the hydroxyl groups of the threonines, making it likely that the threonine face is pointing toward the core. However, such a model has yet to be confirmed, for example, by ^{1}H NMR investigations, which are currently in progress. The bending of the β-sheet due to functional asymmetry of the β-sheet face implies additionally that a ribbon structure (a double tape composed of two β-sheets) is unlikely, because this structure would exhibit two symmetric faces, as was described previously.[14]

From AFM micrographs, the pitch height and the pitch angle could be determined, making the calculation of the maximum tape width of about 13.7 ± 2 nm possible by applying simple trigonometry (cf., Supporting Information). This can be compared to the theoretical width of an antiparallel β-sheet tape that is formed by the conjugate **V**. The tape width could be calculated as ~7.2 nm by considering that the peptide segment adopts a fully extended β-strand with 0.35 nm per amino acid residue[41] and that the polymer forms a statistical coil. It is most likely that the polymer block adopts an extended coil conformation due to the low degree of polymerization and packing constrains. This is also suggested by AFM and TEM measurements, because a gap of about 6.5 nm between the tape slopes should be more evident. However, the fully stretched, all-trans brush conformation of the polymer would be rather unlikely, due to the loss of conformational entropy, even if the width of such a 2D-tape would meet quite exactly the maximum tape width of 13.7 nm.

(38) Aggeli, A.; Bell, M.; Boden, N.; Keen, J. N.; McLeish, T. C. B.; Nyrkova, I.; Radford, S. E.; Semenov, A. *J. Mater. Chem.* **1997**, *7*, 1135−1145.
(39) Hwang, W.; Marini, D. M.; Kamm, R. D.; Zhang, S. *J. Chem. Phys.* **2003**, *118*, 389−397.
(40) Fishwick, C. W. G.; Beevers, A. J.; Carrick, L. M.; Whitehouse, C. D.; Aggeli, A.; Boden, N. *Nano Lett.* **2003**, *3*, 1475−1479.
(41) Stryer, L. *Biochemistry*, 4th ed.; W. H. Freeman and Co.: New York, 1995.

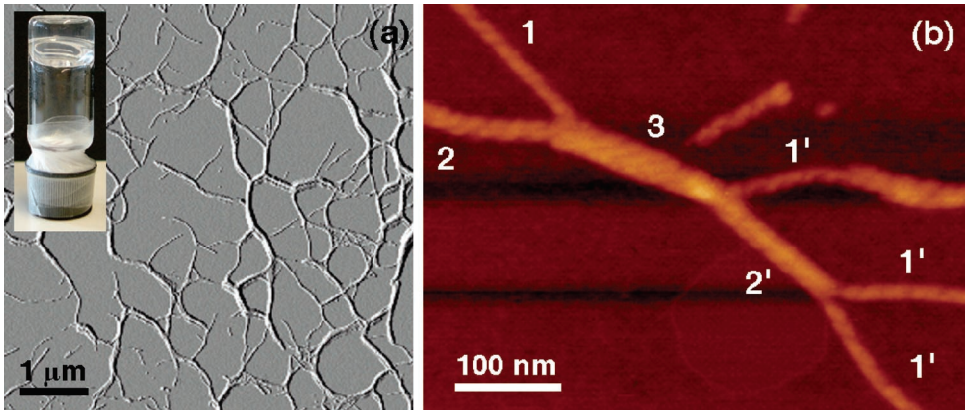

Figure 3. AFM micrograph of the gel structure formed by a solution of **V** (0.6 mmol/L in diethyl ether/methanol (85 vol %)) after 6−12 h cross-linking at room temperature (tapping mode, amplitude $z = 0.2$ V) (a); macroscopic gel after 24 h (a, inset); micrograph of a cross-link in the gel (height image $z = 5$ nm) showing single tapes with helical twist as proto-structures (1,1′), dual tapes (dimers: 2,2′), and trippel tapes (trimers: 3) (b).

Given a structure model that suggests a densely wound, twisted and bent β-sheet tape, the average bending and twisting angles per peptide β-strand can be calculated as described by Aggeli, Boden, and co-workers (cf., Supporting Information).[37] Assuming a cyclic cross section of the superstructure in solution with a calculated radius of about 7.1 nm ($r = \text{circumference}_{\text{ellipsoid}}/2\pi$), the twist and bend angles were calculated as $\gamma_\theta \approx 1.9°$ and $\gamma_\nu \approx 2.3°$, respectively. These can be compared to symmetrical distortion angles of $\gamma_\theta = \gamma_\nu \approx 3°$ published for β-sheet assemblies of 11mer oligopeptides in water.[37] Apparently, in organic solvents a stiffer β-sheet tape is formed, showing a decreased distortion that results in a wound helix with less curvature. This can be expected, due to the differences in binding energy contributions of H-bonds in organic solvents as compared to that in water. Because H-bonds are stronger in diethyl ether, the binding between the β-strands in a β-sheet tape is also stronger. Thus, distortion of the tape, driven by dipole moments and/or chemical anisotropy, is energetically more demanding.[42]

It is a notable feature of the structure-mechanics of β-barrels (a rolled single β-sheet is considered as the simplest β-barrel) that the superstructure is rather stable but not rigid and tolerates sheer deformation. This is supported by the AFM investigations because an anisometric elliptical cross section was found if the superstructures were visualized on a mica substrate. Because such deformation was observed, applying low damping conditions, it would be straightforward to speculate that one of the forces generating the structure deformation results from the strong adsorption of p*n*BA to the mica, as was previously shown with molecular brush systems.[43,44]

As compared to classical polymers, it is a remarkable property of sequence-defined peptides that structures with multiple levels of well-defined, hierarchical order are formed. Along with this, extended β-sheet assemblies have the inherent tendency to organize beyond the secondary structure level. Frequently this is independent of size or complexity of the peptide strands,[45] leading to the formation of double β-sheets (ribbons), fibrils, and fibers, which can span dimensions from the nanometer to the micrometer. Particularly, such assembly processes of β-sheets are currently an important field of medical research, because the amyloid β-protein ($A\beta_{1-42}$) forms dense, intracellular bundles of β-sheet fibrils in the brain during a pathological misfolding. These structures are discussed as pathogenic assemblies involved in the irreversible and progressive neurodegenerative disorder referred to as Alzheimer's disease.[46]

Hence, it is not surprising that the helical superstructures, formed in organic solutions by **V**, exhibit the tendency to self-assemble further and to adopt higher levels of hierarchical order. Microscopically, this can be observed in TEM and AFM micrographs (Figures 2, left, and 3, respectively) that show the aggregation of $n\times$ times of proto-structures (helical superstructure). The resulting bundles exhibit a uniform, left-handed helical twist, which is consistent with models for peptide folding.[37] Moreover, this indicates that the association of the proto-structures follows a defined organization principle. Therefore, a simple statistical entanglement due to lateral, undirected interactions can be excluded. Macroscopically this organization results in the formation of continuous organo-gels from a concentration of $c[\mathbf{V}] = 0.6$ mmol/L (2 mg/mL) within about 6−12 h (cf., Figure 3, inset). The gel structure is comparatively soft, and a gel−fluid transition can be observed under mild sheer stress. This suggests that the cross-linking of the proto-structures occurs due to reversible, soft interactions, making this gel structure suitable for auto-correction, and self-adaptation, which are necessary properties for sensitive responsive materials.

Conclusions

The synthesis and the self-assembly properties of a peptide−polymer conjugate in organic solvents have been described. The conjugate was obtained via solid-phase supported peptide synthesis (SPPS) followed by on-support coupling of a carboxyl end-functionalized poly(*n*-butyl acrylate) (p*n*BA). A strong aggregator domain with a primary structure of $(\text{Thr}-\text{Val})_5-\text{nPhe}-\text{Gly}$ was used as peptide segment to generate a high propensity for adopting the β-sheet secondary structure. A clean synthesis and ease of handling of the conjugate was achieved by the incorporation of two switch defect segments into the $(\text{Thr}-\text{Val})_5$ domain by substituting the amide bonds between $\text{Val}^4-\text{Thr}^5$ and $\text{Val}^8-\text{Thr}^9$ with O^β Thr esters. Thus, the aggregation tendency of the 1,3-switch domain (alternating

(42) Schlaad, H.; Smarsly, B.; Below, I. *Macromolecules* **2006**, *39*, 4631−4632.
(43) Boerner, H. G.; Beers, K.; Matyjaszewski, K.; Sheiko, S. S.; Moeller, M. *Macromolecules* **2001**, *34*, 4375−4383.
(44) Potemkin, I. I.; Khokhlov, A. R.; Prokhorova, S.; Sheiko, S. S.; Moeller, M.; Beers, K. L.; Matyjaszewski, K. *Macromolecules* **2004**, *37*, 3918−3923.
(45) Zhang, S.; Zhao, X. *J. Mater. Chem.* **2004**, *14*, 2082−2086.
(46) Gorman, P. M.; Chakrabartty, A. *Biopolymers* **2001**, *60*, 381−394.

native Val−Thr and switch Val−Thr segments) in the conjugate was fully suppressed in methanol as well as in a diethyl ether/methanol. No secondary structure formation was observed in methanolic solution by circular dichroism (CD) spectroscopy and in the diethyl ether/methanol mixture by infrared (IR) spectroscopy. Moreover, atomic force microscopy (AFM) was providing no evidence for the formation of ordered microstructures in these solvents. However, after performing the O−N−acyl transfer rearrangement in the switch segments, the fully native $(Thr-Val)_5$ domain was re-established. This restores the aggregation tendency of the $(Thr-Val)_5$ domain in the conjugate, and hence triggers self-assembly into antiparallel β-sheets, as confirmed by IR and CD spectroscopy. Moreover, AFM visualizes the formation of rather soft, left-handed helical superstructures with heights of about 2.9 nm, widths of about 10 nm (TEM), and uniform pitch heights of 37 nm. A structure model has been proposed, according to the dimensions of the observed structure and the spectroscopic investigations. The results suggest the formation of a core−shell tape, through the assembly of the peptide segment of the conjugate. Hence, the p*n*BA forms the shell, while the peptide adopts an antiparallel β-sheet in the core. The latter causes the tape to twist and bend due to dipole moments and chemical differences of the two faces of the β-sheet, leading to the formation of the helical superstructure. Further assembly of these proto-structures is observed because reversible cross-linking leads to the formation of rather soft, continuous organo-gels. The mechanism of cross-linking was investigated by AFM. In the assembly process, the helical superstructures (proto-filaments) organize into well-defined helical bundles exhibiting a distinct number of associated proto-filaments (di-, tri-, tetramers) and an expected left-handed helical twist. The presented example demonstrates that the peptide-guided organization can be successfully transferred into organic solvents, and thus opens the possibility to incorporate a broad spectrum of synthetic polymers with different functionalities and mechanical properties. Indeed, this might allow the rational design of synthetic, polymer materials with controlled microstructure that possibly heralds an approach toward functional control in synthetic materials. As an example of such functional peptide-polymer assemblies, nanosprings and nanospring networks have been realized. The micromechanics of these distinct objects and connected networks are currently under investigation.

Experimental Section

The materials, methods, and synthetic procedure for the carboxylate end-functionalized p*n*BA (**III**) are described in detail in the Supporting Information.

Synthesis of II: 1,3-Switch Peptide (H−Thr−Val−Thr−(Val−Thr)^{switch}−Val−Thr−(Val−Thr)^{switch}−Val−nPhe−Gly−OH). A TentaGel polystyrene-(2-chlorotrityl chloride) resin was loaded with Fmoc−Gly OH by following standard protocols, and the loading was determined to be 0.25 mmol/g by an analytical Fmoc test using UV spectroscopy.[47] Before using the preloaded resin (**I**), a capping step was performed applying enforced capping conditions (Ac_2O/NMI/NMP, 2 × 15 min). The subsequent coupling of the standard amino acids, leading to native amide bonds and the removal of the Fmoc protecting groups, was performed on an Applied Biosystems ABI 433a peptide synthesizer, in NMP as the solvent, following standard ABI-Fastmoc, double coupling, and Fmoc deprotection protocols. Fmoc amino acid coupling was facilitated using HBTU/DIPEA in NMP. The synthesis was interrupted after each coupling cycle to verify full conversion with the colorimetric Kaiser test.[48]

The switch esters were synthesized by applying enforced coupling procedures using benchtop procedures as has been described recently.[15] Briefly, the coupling of the Fmoc−Val OH onto the unprotected β-hydroxyl side-chain functionality of the prior attached *t*Boc−Thr OH was accomplished in a glass reactor in DCM. Coupling was facilitated by DIC/NMI, and quantitative conversion was confirmed by analytical Fmoc tests using UV spectroscopy.[47] When necessary, repetitive coupling cycles were carried out to force the coupling reaction to completion. To ensure the absence of deletion sequences, capping steps following Ac_2O/NMI/NMP protocols were performed prior to the removal of the Fmoc amine protecting group. After the (Val−Thr)^{switch} segment was successfully synthesized and the capping step was performed, the resin was washed carefully and transferred to the peptide synthesizer where the synthesis of the native peptide segments proceeded in an automated manner. After final removal of the Fmoc protecting group, a small amount of **II** was liberated from the support to characterize the precursor segment. The cleavage was accomplished by 30 min treatment of the dried resin with a cleavage mixture of TFA/DCM/triethylsilane (50/49/1 vol %). The peptide could be isolated by diethyl ether precipitation, centrifugation, and washing of the precipitate with diethyl ether, followed by lyophilization from 1,4-dioxane.

Analysis of II. ^{1}H NMR (MeOH-d_4 (3.30 and 4.86 ppm)): δ = 0.95−0.98 (m, 30H, C(C*H*$_3$)$_2$ Val), 1.15−1.21 (m, 9H, C(C*H*$_3$)OH Thr), 1.27−1.37 (dd, 6H, C(C*H*$_3$)O−CO Thr), 2.02−2.18 (m, 5H, C*H*(CH$_3$)$_2$ Val), 3.63−4.46 (m, 19H, 12 α-C*H* + 3C*H*−OH Thr + C*H*$_2$–CH nPhe), 5.14−5.22 (dt, 2H, C*H*−O−CO Thr), 7.52−7.55 (d, 2H, C$_{ar}$*H* nPhe), 8.12−8.14 (d, 2H, C$_{ar}$*H* nPhe) ppm. FT-IR: ν = 3281 (w, amide A), 2973−2880 (m, C−H), 1742 (w, C═O ester), 1640 (s, C═O amide I), 1519 (s, amide II), 1346 (m, amide III), 1181−1132 (s, O−H) cm^{-1}. ESI-MS *m*/*z* = 1291 ([M + Na]$^+$), 1269 ([M + H]$^+$), 635 ([M + 2H]$^{2+}$), 626 ([(M − H$_2$O) + 2H]$^{2+}$, Thr in source fragmentation) (cf., the Supporting Information for the MS spectra).

Synthesis of IV: Polymer−Peptide Conjugate (p*n*BA-*block*-Thr−Val−Thr−(Val−Thr)^{switch}−Val−Thr−(Val−Thr)^{switch}−Val−nPhe−Gly−OH). The conjugation of the end-functionalized p*n*BA−COOH (**III**) to the N-terminus of the fully protected peptide segment (**II**) was performed as a solid-phase supported coupling reaction. Selective coupling was achieved by dissolving 640 mg of **III** (0.32 mmol, 4 equiv with respect to the theoretical amount of **II**) in 5 mL of DMF, followed by activation of the carboxyl functionality with PyBOP/HOBt/DIPEA (167 mg, 0.32 mmol, 4 equiv/49 mg, 0.32 mmol, 4 equiv/0.1 mL, 0.64 mmol, 8 equiv). The resulting solution was added to the resin, shaken for 18 h, and subsequently after a washing step the coupling was repeated to achieve quantitative conjugation. This was verified by the colorimetric Kaiser test that indicated complete consumption of the terminal amine functionality of **II**.

The liberation of the conjugate **IV** from the support was accomplished by 2 × 30 min treatment with a cleavage mixture TFA/DCM/triethylsilane (50/49/1 vol %), followed by two washing cycles with the cleavage solution. The conjugate was isolated in 62% yield after precipitation in pentane, followed by drying in a vacuum and lyophilization from 1,4-dioxane.

Analysis of IV. ^{1}H NMR (MeOH-d_4 (3.30 and 4.86 ppm)): δ = 0.94−0.98 (m, 75H, 30H C(C*H*$_3$)$_2$ Val + 46H CH$_2$–C*H*$_3$), 1.11−1.28 (m, 18H, 9H C(C*H*$_3$)OH Thr + 6H C(C*H*$_3$)O−CO Thr + 3H CH−C*H*$_3$ p*n*BA), 1.41 (m, 32H, C*H*$_2$–CH$_3$ p*n*BA), 1.60−1.91 (b, 59H, CH$_2$–C*H*$_2$–CH$_2$ + CH−C*H*$_2$ p*n*BA), 2.16−2.18 (m, 5H, C*H*(CH$_3$)$_2$ Val), 2.31 (b, 15H, C*H*−CH$_2$), 3.63−4.55 (m, 51H, 12H α-C*H* + 3H C*H*−OH Thr + C*H*$_2$–CH nPhe + 32H, O−C*H*$_2$ p*n*BA), 5.16−5.24 (dt, 2H, C*H*−O−CO Thr), 7.53−7.55 (d, 2H, C$_{ar}$*H* nPhe), 8.12−8.14 (d, 2H,

(47) Chan, W. C.; White, P. D. *Fmoc Solid-Phase Peptide Synthesis: A Practical Approach*; Oxford University Press: Oxford, 2000; 346 pp.

(48) Kaiser, E.; Colescot, R.; Bossinge, C.; Cook, P. I. *Anal. Biochem.* **1970**, *34*, 595−599.

$C_{ar}H$ nPhe) ppm. FT-IR: ν = 3292 (w, amide A), 2960−2880 (m, C−H), 1730 (s, C═O ester), 1642 (s, C═O amide I), 1523 (m, amide II), 1346 (m, amide III), 1153 (s, O−H) cm^{-1}.

Aggregation Procedure. Two milligrams (0.6 μmol) of the conjugate (**IV**) was dissolved either in 0.95 mL of methanol or in a mixture of 0.89 mL of diethyl ether and 0.06 mL of methanol. After 0.06 mL of 0.02 M NaOH in MeOH (1.2 μmol of NaOH) was added, the mixture was gently shaken for 12 h. Gel formation took place in ether/methanol after stopping the agitation, within 6−12 h (viscosity increase after ∼3−6 h and continuous gel formation after ∼12 h). To ensure the reproducibility of the conditions during the switch from **IV** → **V** in methanol, the amount of acid present in the methanolic solution (apparent pH value) was estimated by diluting 10 μL of the solution with 3 μL of deionized water and measuring the pH with a standard indicator paper (pH range: 5−8).

Acknowledgment. We thank Dr. Nikolai Severin and Prof. Jürgen Rabe (HU Berlin) for support during AFM measurements, Prof. Markus Antonietti for his continued support and helpful discussions, and Andrea Grafmüller for the artwork. Hartmut Rettig, Jessica Brandt, Katharina Ostwald, Anne Heilig, and Marlies Gräwert are thanked for their contributions to this project. Financial support was granted from the German Research Foundation through the Emmy Noether Program (BO1762/2) and the Max Planck Society.

Supporting Information Available: Materials, methods, and synthetic procedure of the end-functionalized p*n*BA (**III**); mass spectrum of the peptide **II**. Characterization of the aggregation behavior of **IV** and **V** (CD, AFM, and FT-IR). This material is available free of charge via the Internet at http://pubs.acs.org.

JA0649872